

Modeling Cement Hydration Kinetics Using the Equivalent Age Concept

Xueyu Pang¹, Dale P. Bentz², Christian Meyer¹

1: Dept. of Civil Engineering and Engineering Mechanics, Columbia University, USA

2: Engineering Laboratory, National Institute of Standards and Technology, USA

In this study the hydration kinetics of four different types of cements during early ages were investigated by both chemical shrinkage and isothermal calorimetry tests. Chemical shrinkage tests were performed at both different temperatures and pressures while isothermal calorimetry tests were conducted only at different temperatures. The hydration kinetics curves at different curing conditions converged reasonably well if properly transformed with a set of scaling factors. Therefore, the experimental hydration kinetics curve at one curing condition can be used to predict that of another curing condition using a single scale factor. The scale factor is similar to the coefficient used to compute the equivalent age of a specified curing condition when applying the maturity method to estimate concrete strength. Its dependence on curing temperature and curing pressure can be modeled by the activation energy and the activation volume of the cement, respectively.

Keywords: hydration kinetics, temperature, pressure, chemical shrinkage, heat evolution, oil well cement

1 Introduction

Cement hydration is a complex chemical process that involves a number of different reactions. Although many detailed features of the process are still not clearly understood today, the general hydration kinetics can be approximately represented by the overall degree of hydration as a function of time. This overall degree of cement hydration, defined as the total weight fraction of cement reacted, is directly related to many different physical and mechanical properties of cement-based materials, such as viscosity [1], setting time [2-4], autogenous shrinkage [5], compressive strength [6, 7], tensile strength [8], and modulus of elasticity [5, 8]. It is arguably the most important parameter that can be used to model the time-dependent characteristics of cement-based materials [9]. Since Portland cement mainly consists of four clinker phases, its overall degree of hydration can be written as [10]:

$$\alpha(t) = p_{C_3S}\alpha_{C_3S}(t) + p_{C_2S}\alpha_{C_2S}(t) + p_{C_3A}\alpha_{C_3A}(t) + p_{C_4AF}\alpha_{C_4AF}(t) \quad (1)$$

where p_i is the original weight fraction of *Phase i* in the anhydrous cement and $\alpha_i(t)$ is the degree of hydration of *Phase i* at time t . Direct determination of $\alpha_i(t)$ can be made by using quantitative X-ray diffraction analysis [10, 11], but the method is rarely used in practice due to complex test procedures and high equipment cost.

Some properties of a hydrating cement paste, such as the cumulative heat evolution, the total chemical shrinkage, and the non-evaporable water content, have been shown to have approximately linear relationships with each other and the overall degree of hydration [4, 10, 12, 13]. These properties therefore provide indirect ways of determining $\alpha(t)$. As a matter of fact, α is more commonly determined by these indirect methods due to their simplicity. The following equation may be used to convert experimental results to the degree of hydration of cement:

$$\alpha(t) = \frac{H(t)}{H^0} = \frac{CS(t)}{CS^0} = \frac{w_n(t)}{w_n^0} \quad (2)$$

where $H(t)$ and H^0 are the amounts of cumulative heat evolution at time t and at complete hydration, respectively (typically in J/g cement); $CS(t)$ and CS^0 are the amounts of chemical shrinkage at time t and at complete hydration, respectively (typically in mL/g cement); while $w_n(t)$ and w_n^0 are the non-evaporable water contents at time t and at complete hydration,

respectively (typically in g/g cement). It should be pointed out that the hydration reactions of different phases in Portland cement have different contributions toward the overall parameters (i.e. $H(t)$, $CS(t)$, and $w_n(t)$). Since these reactions progress at different rates (that also vary with time), the indirect methods only give a gross approximation to the total hydration kinetics.

Among the different methods of evaluating cement hydration kinetics, heat evolution measured by isothermal calorimetry tests used to be the only ones that give continuous test results (i.e. hydration kinetics curves). In recent years, several new chemical shrinkage test methods have been developed, which also give continuous test results [14-17]. Hydration kinetics curves are most commonly represented by two types of curves: total degree of hydration vs. time (defined here as the integral curve) and rate of hydration vs. time (defined here as the derivative curve). According to Eq. (2), estimating the parameters at the complete hydration condition (i.e. H^0 and CS^0) is essential for converting experimental data to degree of hydration. The cumulative heat evolution of cement at complete hydration mainly depends on the cement compound composition and may be estimated in units of J/g cement by the following equation [17],

$$H^0 = 510p_{C_3S} + 247p_{C_2S} + 1356p_{C_3A} + 427p_{C_4AF} + 239p_{C_2F} \quad (3)$$

The total chemical shrinkage at complete hydration is more difficult to estimate because it depends on both cement composition and curing condition. By studying the correlations between chemical shrinkage and non-evaporable water content, the following equations were proposed to estimate the total chemical shrinkage at complete hydration [17]:

$$CS^0 = w_n^0 (v_w - v_n) \quad (4)$$

$$w_n^0 = 0.257p_{C_3S} + 0.217p_{C_2S} + 0.56p_{C_3A} + 0.202p_{C_4AF} + 0.113p_{C_2F} \quad (5)$$

where v_w and v_n are the specific volumes (cm^3/g) of capillary water and non-evaporable water in cement pastes, respectively, both of which depend on curing condition. For the ambient condition (25 °C, 0.101 MPa), it was estimated that $v_w = 0.988 \text{ cm}^3/\text{g}$ and $v_n = 0.752 \text{ cm}^3/\text{g}$.

2 Experimental materials and methods

Four different classes of oil well cements (American Petroleum Institute (API) Specification 10A [18]), namely Class A, C, G, and H cements, were used here to study hydration kinetics. The main potential compound compositions of the different types of cement (derived from the oxide analysis test results using the Bogue calculation method) are listed in Table 1. The specific surface areas of Class A, C, G, and H cements calculated from the PSD data (assuming spherical cement particles with a density of 3150 m^3/kg) were 356.2 m^2/kg , 564.9 m^2/kg , 326.5 m^2/kg , and 393.9 m^2/kg , respectively. It is obvious that Class C cement was ground much finer than the other classes to achieve a higher specific surface area. Neat cement slurries were prepared with standard water-to-cement (w/c) ratios for each class of cement, as defined in API Specification 10A [18]. More detailed information about the properties of these cements as well as cement slurry preparation procedures is given in [17]. Note that only one type (premium) of Class H cement is used in this study.

Table 1: Estimated main compound compositions of the different types of cements (mass %)

Cement	C ₃ S	C ₂ S	C ₃ A	C ₄ AF	C ₂ F	CaSO ₄	Free Lime
A	61.66	12.01	8.36	9.41	0	4.67	1.43
C	72.24	5.21	2.16	11.82	0	4.74	0.23
G	62.62	15.90	4.80	10.87	0	3.84	0.21
H	47.91	27.46	0	16.17	1.97	4.21	0.30

Two main test series will be discussed. In test series I, hydration kinetics of the cements is measured by isothermal calorimetry tests using an isothermal calorimeter according to standard test procedures [19]. Tests were conducted at atmospheric pressure and three different curing temperatures. Table 2 shows the test scheme for this test series. The temperatures of isothermal calorimetry tests can be controlled precisely due to the small sample size (4 ~ 5 g). For this technique, the average absolute difference between replicate specimens of cement paste is 2.4×10^{-5} W/g (cement), with a maximum absolute difference of 0.00011 W/g (cement), for measurements conducted between 1 h and 7 d after mixing [20].

Table 2: Isothermal calorimetry tests (test series I, test age = 168 hours)

Curing Temperature (°C)		25	40	60
Cement	w/c	-	-	-
A	0.46	A-25	A-40	A-60
C	0.56	C-25	C-40	C-60
G	0.44	G-25	G-40	G-60
H	0.38	H-25	H-40	H-60

In test series II, hydration kinetics of the cements is measured by chemical shrinkage tests using an innovative test apparatus consisting of pressure cells and syringe pumps. Detailed descriptions of the test apparatus and test procedures are given in [17]. Chemical shrinkage tests were performed under both different curing temperatures and pressures. The test scheme is shown in Table 3. The advantages of the new test apparatus are that it allows easy application of hydrostatic pressure and that it appears to eliminate the dependence of test results on specimen thickness. The main shortcoming of the new apparatus is the lack of precise temperature control. Test data oscillation seems to be dramatically increased when heat controllers are used to control the temperature of the specimens, which usually prevents reliable derivative curves to be directly obtained from experimental data. As shown in Table 3, a majority of the tests in this test series were conducted at lab temperatures without using the heat controllers such that derivative curves could be obtained. Due to lab temperature fluctuations, it is very difficult to produce exact replicate specimens at ambient temperatures. The lab temperatures at the beginning of each test were recorded for later calibrations (temperature fluctuations during the period of a single test were typically within ± 1.1 °C). Uncertainties in test results caused by factors other than temperature fluctuations are estimated to be less than 3% at the end of 3 days. More detailed uncertainty analysis of this experimental technique is given in [17].

Table 3: Chemical shrinkage tests (test series II, test age = 72 hours)

Curing Temperature (°C)		Ambient ^a				40.6 ^b	60 ^b
Curing Pressure (MPa)		0.69	17.2	34.5	51.7	0.69	0.69
Cement	w/c	-	-	-	-	-	-
A	0.46	A-1	A-2	A-3	A-4	A-5	A-6
C	0.56	C-1	C-2	C-3	C-4	C-5	C-6
G	0.44	G-1	G-2	G-3	G-4	G-5	G-6
H	0.38	H-1	H-2	H-3	H-4	H-5	H-6

^a: Lab temperature (~ 24 °C ± 2.8 °C).

^b: Estimated cement specimen temperature.

3 Model formulation

In ASTM standard 1074 [7], maturity is defined as the extent of the development of a property of a cementitious mixture and equivalent age is defined as the number of days or hours at a specified temperature required to produce a maturity equal to the maturity achieved by a curing period at temperatures different from the specified temperature. The maturity function used to compute the equivalent age at a specified (reference) temperature is as follows [7],

$$t_r = \sum \exp\left(-\frac{E_a}{R}\left(\frac{1}{T} - \frac{1}{T_r}\right)\right) \cdot \Delta t \quad (6)$$

where t_r (h) is the equivalent (reference) age at the reference temperature T_r (K); E_a (J/mol) is the activation energy of the cement; R is the gas constant; and T (K) is the average temperature during time interval Δt (h). For isothermal curing conditions (T is constant over time), Eq. (6) becomes,

$$t_r = \exp\left(\frac{E_a}{R}\left(\frac{1}{T_r} - \frac{1}{T}\right)\right) \cdot t = C \cdot t \quad (7)$$

where t is the actual age at temperature T ; C is a scale factor, which is a function of T_r and T . Eq. (7) means that the maturity achieved at age t at curing temperature T is the same as that achieved at age Ct at curing temperature T_r . For the purpose of modeling cement hydration kinetics, maturity can be interpreted here as the degree of hydration of cement. Therefore, if the hydration kinetics at the reference temperature T_r is represented by the following unknown functions

$$\text{Integral curve: } \alpha = f(t), \text{ Derivative curve: } d\alpha / dt = f'(t) \quad (8)$$

then the hydration kinetics at temperature T can be represented by

$$\text{Integral curve: } \alpha = f(Ct), \text{ Derivative curve: } d\alpha / dt = C \cdot f'(Ct) \quad (9)$$

The maturity function (Eq. (6)) is developed based on the Arrhenius equation, which is one of the basic chemical kinetics laws describing the temperature dependence of the reaction rate constant. Therefore, the results shown in Eqs. (8) and (9) are the same as those derived from chemical kinetics theories [17]. When the pressure dependence of the reaction rate constant is also taken into account, the scale factor should be written as [17],

$$C = \exp\left(\frac{E_a}{R}\left(\frac{1}{T_r} - \frac{1}{T}\right) + \frac{\Delta V^\ddagger}{R}\left(\frac{P_r}{T} - \frac{P}{T}\right)\right) \quad (10)$$

where ΔV^\ddagger is the activation volume of the cement; P is the actual curing pressure; and P_r is the specified (reference) curing pressure.

4 Test results and discussion

To convert heat evolution and chemical shrinkage test results to degree of hydration data, the conversion factors (i.e. H^0 and CS^0) for different cements must be estimated. H^0 can be obtained by substituting the cement composition data listed in Table 1 into Eq. (3). The total heat evolution at complete hydration (H^0) of the Class A, C, G, and H cements used in this study are determined to be 497.7 J/g, 461.1 J/g, 470.1 J/g, and 385.9 J/g, respectively. For ambient curing temperature (25 °C), CS^0 can be estimated by substituting the cement composition data into Eqs. (4) and (5). The variations of v_w and v_n with pressure can be estimated by assuming that capillary water has the same bulk modulus as fresh water and that non-evaporable water has a bulk modulus of 10.6 GPa [17]. The variation of v_n with curing

temperature is still uncertain, making it difficult to estimate CS^0 at different temperatures. However, within the range studied here, CS^0 may be assumed to decrease approximately linearly with increasing temperature. The linear reduction rate varies slightly with cement composition and is estimated to be 0.63 %, 0.66 %, 0.59 %, and 0.75 % per °C for the Class A, C, G, and H cements, respectively [17]. The calculated values of CS^0 at different curing conditions are listed in Table 4. Figure 1 and Figure 2 show some representative hydration kinetics test results measured by isothermal calorimetry and chemical shrinkage tests, respectively. It is obvious that hydration rate increases with both increasing curing temperature and increasing curing pressure, especially at early ages. Figure 2 also suggests that a relatively large pressure increase is comparable to only a small temperature increase, in terms of its effect on the rate of hydration. For tests conducted at ambient temperatures (Table 3), hydration kinetics test results reflect both the effect of curing pressure and temperature since the lab temperatures of these tests are not exactly the same.

Table 4: Total chemical shrinkage at complete hydration (mL/100g)

Temperature (°C)	25	25	25	25	25	40.6	60
Relative Pressure (Mpa)	0	0.69	17.2	34.5	51.7	0.69	0.69
A	5.914	5.906	5.756	5.606	5.468	5.326	4.604
C	5.505	5.498	5.358	5.218	5.090	4.932	4.228
G	5.771	5.763	5.617	5.470	5.335	5.233	4.573
H	5.140	5.133	5.003	4.872	4.752	4.533	3.786

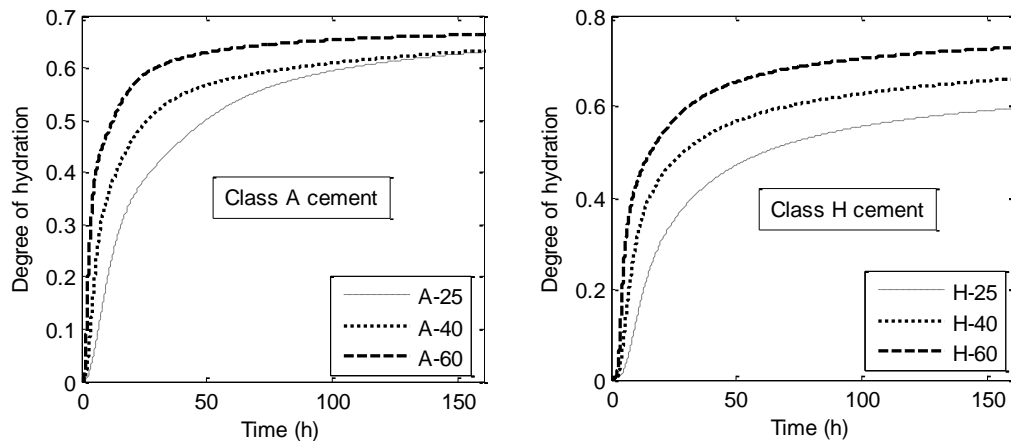


Figure 1: Representative hydration kinetics test results measured by isothermal calorimetry

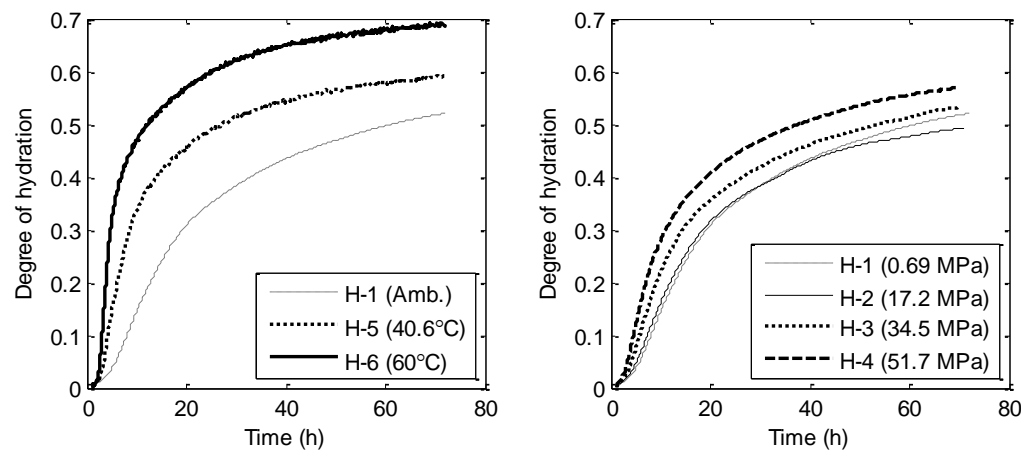


Figure 2: Representative hydration kinetics test results measured by chemical shrinkage

Theoretically, based on the analysis in Section 3, the hydration kinetics curves at different curing conditions should converge when they are normalized by plotting the degree of hydration as a function of the equivalent age using the same reference curing condition. Therefore, the scale factor C associated with a particular curing condition may be estimated by trial and error such that its normalized hydration kinetics curve has the best agreement with the reference curve. Due to the fact that Portland cement is essentially a mixture of several different compounds, which hydrate at different rates and have different sensitivities to curing temperatures and pressures, the normalized hydration kinetics curves for different curing conditions usually do not converge perfectly. In addition, it is often necessary to slightly offset the curve to achieve the best agreement. In other words, a more accurate representation of Eq. (9) is as follows,

$$\text{Integral curve: } \alpha = f(C(t-t_0)), \text{ Derivative curve: } d\alpha/dt = C \cdot f'(C(t-t_0)) \quad (11)$$

where t_0 is the offset time. Such offset is primarily due to the variation of the induction period between different tests, which are affected by many different factors and hence very difficult to model. In this study, the induction period (and the obtained offset value) is also affected by experimental artifacts because cement pastes are not mixed in-situ and it takes time for their temperatures to reach equilibrium. Therefore, for practical purposes, the small offset may be accepted as experimental errors and Eq. (9) should be used to predict hydration kinetics. Table 5 shows the scale factors and offset time obtained for isothermal calorimetry tests. The activation energies of different cements can be calculated using linear regression analyses according to Eq. (10). The values obtained for Class A, C, G, and H cements are 40.3 kJ/mol, 36.9 kJ/mol, 40.1 kJ/mol, and 35.4 kJ/mol, respectively. Table 6 shows the scale factors and offset time obtained for chemical shrinkage tests. The correspondingly determined activation energies of Class A, C, G, and H cements are 43.2 kJ/mol, 40.1 kJ/mol, 40.1 kJ/mol, and 44.1 kJ/mol, respectively. These values are less accurate than those calculated from isothermal calorimetry tests due to the relatively poor temperature control scheme of chemical shrinkage tests. It appears that offset is not necessary for tests conducted at different curing pressures (i.e. $t_0 = 0$). As the ambient (lab) temperatures of the tests conducted at different pressures are not exactly the same, it is important to separate the temperature influences when calculating the activation volumes of the cements. After calibrating for the ambient temperature fluctuations (Table 6) according to Eq. (10), the activation volumes of Class A, C, G, and H cements are estimated to be $-20.8 \text{ cm}^3/\text{mol}$, $-27.5 \text{ cm}^3/\text{mol}$, $-20.1 \text{ cm}^3/\text{mol}$, and $-24.5 \text{ cm}^3/\text{mol}$, respectively.

Table 5: Best-fit scale factors (C) and offset time (t_0) for test series I ($\hat{\cdot}$: reference tests)

Test	A-25 [*]	A-40	A-60	C-25 [*]	C-40	C-60	G-25 [*]	G-40	G-60	H-25 [*]	H-40	H-60
t_0 (h)	0	0.4	0.8	0	0.75	1	0	0.9	1	0	1	1.5
C	1	2.1	5.5	1	2.18	4.8	1	2.3	5.5	1	2.15	4.5

Table 6: Ambient temperatures, best-fit scale factors (C) and offset time (t_0) for test series II ($\hat{\cdot}$: reference tests)

Test	A-1 [*]	A-2	A-3	A-4	A-5	A-6	C-1 [*]	C-2	C-3	C-4	C-5	C-6
$T_{amb.}$ (°C)	24.4	22.8	25	24.4	-	-	26.9	27.5	25	25.6	-	-
t_0 (h)	0	0	0	0	0.7	1	0	0	0	0	0.6	1.2
C	1	1	1.4	1.5	2.7	6.5	1	1.18	1.38	1.6	2.2	5
Test	G-1 [*]	G-2	G-3	G-4	G-5	G-6	H-1 [*]	H-2	H-3	H-4	H-5	H-6
$T_{amb.}$ (°C)	25	24.7	23.1	25	-	-	25.6	22.2	23.9	26.1	-	-
t_0 (h)	0	0	0	0	1	1	0	0	0	0	1	1.7
C	1	1.2	1.18	1.55	2.4	5.5	1	1.02	1.3	1.7	2.5	6.3

As shown in Figures 3, 4, and 5, the normalized hydration kinetics curves at different curing temperatures and pressures converge reasonably well for each type of cement (after offset). The error associated with the offset (which ranges from 0 to 1.7 hours) is only significant during early stages of hydration and becomes negligible when long-term properties are concerned. Test results of different pressures (Figure 5) seem to have better convergences than those of different temperatures (Figures 3 and 4), probably because curing pressure has relatively small effect on hydration kinetics compared to curing temperature for the range studied here. The convergences of the curves suggest that the hydration kinetics curves at various curing conditions can be approximately predicted from that of a reference curing condition using a simple scale factor of C , which can be estimated from Eq. (10). Examples of such predictions are given in [17].

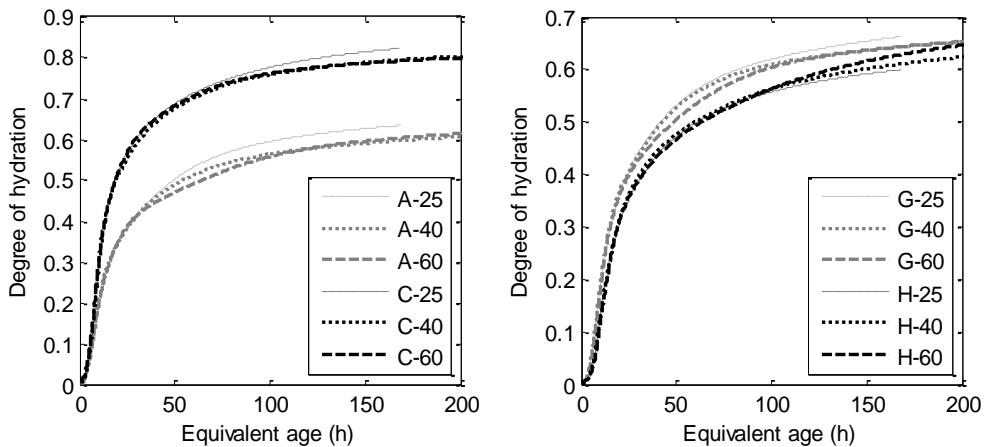


Figure 3: Normalized hydration kinetics curves of different tests (test series I)

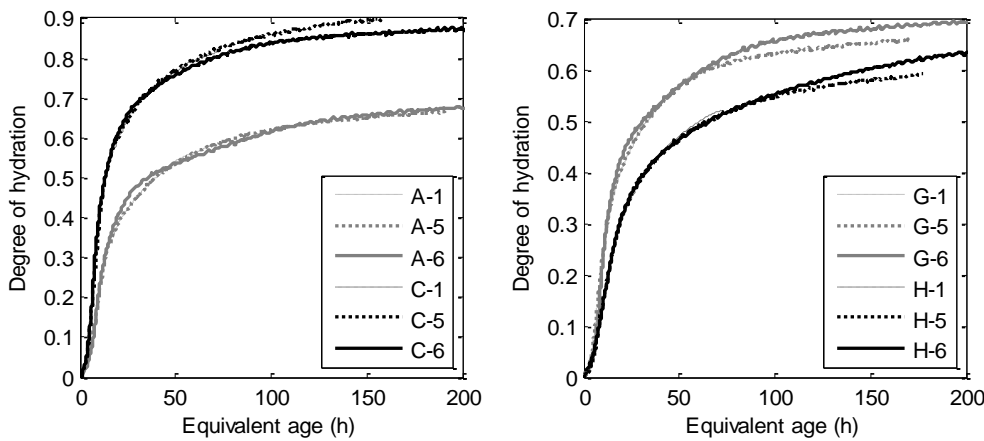


Figure 4: Normalized hydration kinetics curves of different tests (test series II)

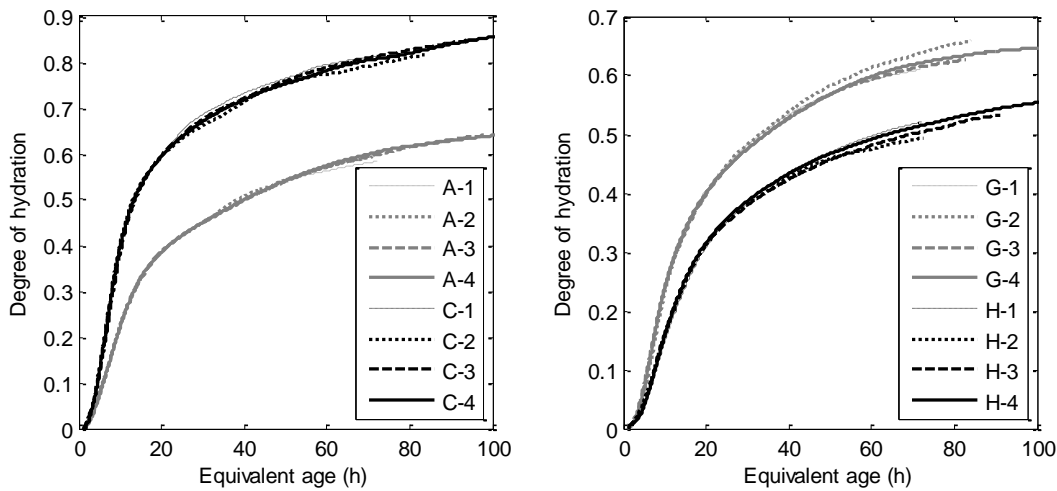


Figure 5: Normalized hydration kinetics curves of different tests (test series II)

5 Conclusions

A simple mathematical model is proposed in this study to model the effect of curing temperature and pressure on cement hydration kinetics. The model is developed based on a similar principle as the equivalent age concept used to compute the maturity of cement-based materials. The model suggests that the hydration kinetics of a given cement at various curing conditions can be approximately predicted from an experimental curve obtained for a reference curing condition using a simple scale factor related to the chemical properties of the cement. However, since the induction period can not be predicted accurately, sometimes a slight offset in the time axis between the predicted curve and the actual experimental curve may be observed.

References

- [1] Scherer, G.W., G.P. Funkhouser, S. Peethamparan, Effect of pressure on early hydration of class H and white cement, *Cement and Concrete Research*, V. 40, pp. 845-850, 2010.
- [2] Pinto, R.C.A. and K.C. Hover, Application of maturity approach to setting times, *ACI Materials Journal* 96, pp. 686–691, 1999.
- [3] García, Á., D. Castro-Fresno, and J.A. Polanco, Maturity approach applied to concrete by means of Vicat tests, *ACI Materials Journal* 105 (5), pp. 445-450, 2008.
- [4] Zhang, J., E.A. Weissinger, S. Peethamparan, G.W. Scherer, Early hydration and setting of oil well cement, *Cement and Concrete Research* 40, pp. 1023-1033, 2010.
- [5] Lin, F., *Modeling of Hydration Kinetics and Shrinkage of Portland Cement Paste*, Ph.D. Dissertation, Columbia University, 2006.
- [6] Kjellsen, K.O., R.J. Detwiler, and O.E. GjØrv, Development of microstructures in plain cement pastes hydrated at different temperatures, *Cement and Concrete Research* 21, pp. 179-189, 1991.
- [7] ASTM C1074, *Standard Practice for Estimating Concrete Strength by the Maturity Method*, ASTM International, West Conshohocken, PA, 2010
- [8] Krauss, M. and H. Karim, Determination of initial degree of hydration for improvement of early-age properties of concrete using ultrasonic wave propagation, *Cement & Concrete Composites* 28, pp. 299-306, 2006.
- [9] Pane, I. and W. Hansen, Concrete hydration and mechanical properties under nonisothermal conditions, *ACI Materials Journal* 99 (6), pp. 534-542, 2002.
- [10] Parrott, L.J., M. Geiker, W.A. Gutteridge and D. Killoh, Monitoring Portland cement hydration: comparison of methods, *Cement and Concrete Research* 20, pp. 919-926, 1990.
- [11] Escalante-Garcia, J.I. and J.H. Sharp, Effect of temperature on the hydration of the main clinker phases in Portland cements: Part I, neat cements, *Cement and Concrete Research* 28 (9), pp. 1245-1257, 1998.

- [12] Bentz, D.P., A three-dimensional cement hydration and microstructure program: I. hydration rate, heat of hydration, and chemical shrinkage, NISTIR 5756, U.S. Department of Commerce, Washington DC, 1995.
- [13] Escalante-Garcia, J.I., Nonevaporable water from neat OPC and replacement materials in composite cements hydrated at different temperatures, *Cement and Concrete Research* 33 (11), pp. 1883-1888, 2003.
- [14] Geiker, M., Studies of Portland cement hydration: measurements of chemical shrinkage and a systematic evaluation of hydration curves by means of the dispersion model, Ph.D. Thesis, Technical University of Denmark, 1983.
- [15] Mounanga, P., V. Baroghel-Bouny, A. Loukili, A. Khelidj, Autogenous deformations of cement pastes: Part I. Temperature effects at early age and micro-macro correlations, *Cement and Concrete Research* 36 (2006) 110-122.
- [16] Peethamparan, S., E. Weissinger, J. Vocaturo, J. Zhang, and G. Scherer, Monitoring chemical shrinkage using pressure sensors, *Advances in the Material Science of Concrete*, ACI SP-270, Vol. 7 (2010), 77-88.
- [17] Pang, X., Effects of curing temperature and pressure on the chemical, physical, and mechanical properties of Portland cement, Ph.D. Dissertation, Columbia University, 2011.
- [18] API Specification 10A, Specification for Cements and Materials for Well Cementing, American Petroleum Institute, 2010.
- [19] ASTM C1679, Standard Practice for Measuring Hydration Kinetics of Hydraulic Cementitious Mixtures Using Isothermal Calorimetry, ASTM International, West Conshohocken, PA, 2009.
- [20] Bentz, D.P., and Ferraris, C.F., Rheology and setting of high volume fly ash mixtures. *Cement and Concrete Composites* 32 (4), pp. 265-270, 2010.